

# Effects of Coil Embolization on the Haemodynamic Variables in a Cerebral Aneurysm

Sophia Tay

**Abstract**—This paper uses computational fluid dynamics to investigate the changes in haemodynamics in coiled and uncoiled cerebral aneurysms. Specifically, the variables investigated include wall shear stress, static pressure, and velocity magnitude. In addition, comparisons are made between modelling the blood flow through the aneurysm as Newtonian fluid flow as opposed to non-Newtonian. This review aims to contribute to a deeper understanding of endovascular coiling, and foster avenues for further research. A simplified aneurysm model is simulated using ANSYS Fluent, and the results are presented through contour plots, x-y graphs, and path line plots. It was concluded that modelling blood with non-Newtonian flow gave significantly more realistic results which align with previous research and blood flow theory. Furthermore, by comparing the coiled and uncoiled aneurysm simulations, it was found that both the wall shear stress and static pressure in the aneurysm decreased after the implementation of a coil, reducing high-flow effects that could cause the aneurysm to rupture. However, the average velocity magnitude in the aneurysm decreased, increasing low flow effects. This is an important finding, as it suggests that although endovascular coiling is a common method of treatment, it comes with a risk that it could exacerbate the situation.

**Index Terms**— Cerebral Aneurysm, Computational Fluid Dynamics, Endovascular Coiling, Wall Shear Stress, Newtonian Fluid

## I. INTRODUCTION

THIS document provides an overview of a study into the effect of endovascular coiling on the hemodynamics within a cerebral aneurysm. The aim of the study is to explore the effect of endovascular coiling on 3 haemodynamic variables in the aneurysm: wall shear stress (WSS), static pressure, and velocity magnitude. According to prior research, aneurysm rupture is ‘the consequence of the inability of the wall to contain the force of the flowing blood’ [1]. Investigating the changes in these variables when an aneurysm is coiled can provide insight into the effectiveness of endovascular coiling as a method of treatment. The study also compares the use of a Newtonian fluid as opposed to a non-Newtonian fluid when simulating blood flow. For this study, a model of an idealized aneurysm

found at a the bifurcation of a main vasculature branch was simulated using ANSYS Fluent’s 2D double precision steady state solver.

### A. Cerebral Aneurysm and Coiling

A cerebral aneurysm is formed when the walls of an artery weaken, causing it to bulge out [2]. If left untreated, this abnormal protrusion can continue to grow until the walls of the vessel are no longer able to withstand the internal stresses, and the aneurysm ruptures. This causes life-threatening issues such a hemorrhage and brain damage.

One common method of treating a cerebral aneurysm, whether than is preventing it from rupturing or from continuing to bleed, is through endovascular coiling. This method involves the insertion of a compact, thin, spring-like platinum metal into the aneurysm [3]. As a result, blood flow into the aneurysm, along with the risk of the aneurysm rupturing, can be reduced. Fig. 1 illustrates an example of a coiled aneurysm.

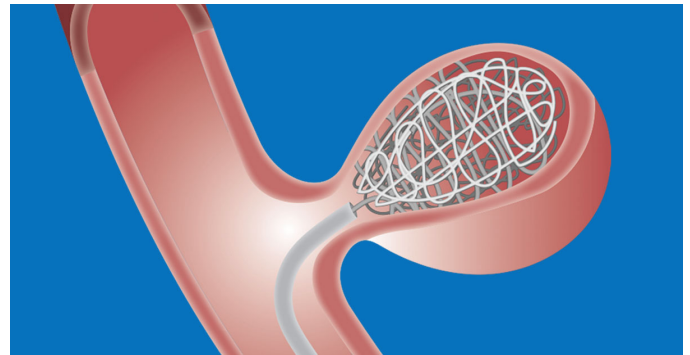


Fig. 1. Coiled Aneurysm [4]

The causes of aneurysm rupture can be divided into two categories: ‘high flow effects’ and ‘low flow effects’ [5]. High-flow effects primarily refer to fast flow, high blood pressure and high levels of WSS causing aneurysm rupture. In contrast, low-flow effects refer to the accumulation of red blood cells, platelets, and leukocytes when blood flows

slower [1]. This can initiate an inflammation process which ultimately leads to the degradation of the aneurysm wall, causing it to rupture. For this investigation, WSS and static pressure were chosen as dependent variables to study the high-flow effects, and velocity magnitude was chosen to study low flow effects.

### B. Computational Fluid Dynamics and Navier-Stokes Equations

Computational Fluid Dynamics (CFD) is the use of numerical methods to simulate fluid-flow and heat-transfer phenomena. ANSYS Fluent is the chosen CFD software for this investigation. It is a numerical solver which solves approximations to the Navier-Stokes Equations, a set of partial differential equations which govern fluid-flow phenomena. These equations describe the conservation of mass, momentum, and energy. For this study, the flow is incompressible and 2D, thus, a simplified form of the Navier-Stokes equations can be solved; these equations are as follows [6]:

#### Conservation of Mass (Continuity)

$$\frac{\partial u}{\partial x} + \frac{\partial v}{\partial y} = 0 \quad (1)$$

#### Conservation of Momentum (x-direction)

$$\rho \left( u \frac{\partial u}{\partial x} + v \frac{\partial u}{\partial y} \right) = -\frac{\partial p}{\partial x} + \mu \left( \frac{\partial^2 u}{\partial x^2} + \frac{\partial^2 u}{\partial y^2} \right) \quad (2)$$

#### Conservation of Momentum (y-direction)

$$\rho \left( u \frac{\partial v}{\partial x} + v \frac{\partial v}{\partial y} \right) = -\frac{\partial p}{\partial y} + \mu \left( \frac{\partial^2 v}{\partial x^2} + \frac{\partial^2 v}{\partial y^2} \right) \quad (3)$$

where the variables are defined as:

$u$  =  $x$  component of velocity (m/s)

$v$  =  $y$  component of velocity (m/s)

$\rho$  = density (kg/m<sup>3</sup>)

$p$  = pressure (Pa)

$\mu$  = viscosity (kg/m·s)

Using (1), (2) and (3), the unknowns ( $u, v, p$ ) can be solved for. In this specific case, the Conservation of Energy equation can be decoupled from the other 3 equations and solved separately.

To approximate the solutions to these equations, ANSYS fluent uses the Finite Volume Method (FVM). This method divides the problem domain into a grid made up of discrete control volumes. Then, it calculates the fluxes of the

conservation quantities across the control volume faces, maintaining conservation principles within each volume.

### C. Assumptions

For this study, several assumptions are made to simplify the model of the aneurysm. First, the aneurysm is modelled in 2D to reduce computational time. Second, the exterior walls of the blood vessels are modelled as rigid, rather than being flexible and able to recoil to accommodate for changes in blood pressure [7]. Third, the aneurysm is modelled to have symmetrical, elliptical geometry, when this symmetry is not guaranteed.

Furthermore, as the inlet velocity of the fluid is very slow, set to be 0.27 m/s, the flow can be assumed to be incompressible. It is also assumed to have constant density and viscosity, and reaches a steady state. This allows ANSYS Fluent to use the incompressible set of Navier-Stokes Equations. The body forces acting on the flow (i.e., gravity) also considered to be negligible. It is also assumed that the model follows the no slip condition, meaning there is no relative motion between the fluid and a wall.

## II. NUMERICAL METHODS

### A. Overview

The study explores 4 cases:

Case 1: An uncoiled aneurysm, modelled with Newtonian fluid.

Case 2: A coiled aneurysm, modelled with Newtonian fluid.

Case 3: An uncoiled aneurysm, modelled with non-Newtonian fluid.

Case 4: A coiled aneurysm, modelled with non-Newtonian fluid.

All cases are modelled with physiological flow.

The coil is modelled by defining the aneurysm region as a porous zone: this type of modelling is called ‘Porous media CFD’, and has been used in recent research to simulate aneurysm treatment [8]. The porosity of a region is given by:

$$\varphi = \frac{V_{void}}{V_{tot}} \quad (4)$$

where  $V_{void}$  is volume of void space in the region, and  $V_{tot}$  is the total volume of the region [9]. By making the aneurysm a porous zone with porosity  $< 1$ , the assumption is made that the coil reduces flow into the aneurysm.

For the Newtonian cases, the fluid has constant viscosity which is independent of shear stress. The relationship between viscosity and shear stress ( $\tau$ ) is given by:

$$\tau = \mu \left( \frac{\partial u}{\partial y} \right) \quad (5)$$

where  $\left(\frac{\partial u}{\partial y}\right)$  is the rate of deformation.

However, blood is a non-Newtonian fluid, and the shear stress is not directly proportional to the rate of deformation. Blood is a pseudoplastic fluid, which means its viscosity decreases with increasing shear stress, and vice versa [10]. This is an important characteristic of blood as it allows it to flow through different sized capillaries. For the non-Newtonian cases, the Blood Power Law [11] is used as to define the non-Newtonian viscosity:

$$\eta = k\dot{\gamma}^{n-1}H(T) \quad (6)$$

where:

$\eta$  = non-Newtonian viscosity (kg/m·s)

$n$  = power law index, an indication of how far the fluid deviates from Newtonian behavior

$k$  = flow consistence index (kg·s<sup>n-2</sup>/m), a measure of the average viscosity of the fluid [12]

$\gamma$  = weight per unit volume (N/m<sup>3</sup>)

$T$  = temperature (K)

However, in this model, non-Newtonian viscosity is assumed to be independent of temperature.

## B. Methodology

The steps below outline the methodology used to simulate the project. Note that some steps differ for the uncoiled/coiled case, as well as for the Newtonian/non-Newtonian case.

### 1) Grid Independence Study

To determine the ideal number of mesh elements for the simulation and to demonstrate that the results of the simulations are grid independent, a parametric study was conducted (method derived from [13]). An ‘ideal number’ of mesh elements is one which gives accurate results, while also not taking up an irrational amount of computational time. Using ANSYS Fluent’s “Parameters” feature, the average outlet velocity, average aneurysm WSS, and average intra-aneurysmal static pressure was calculated for different numbers of mesh elements. This data was then analyzed to optimize the number of mesh elements used.

### 2) Create Model Geometry

Using ANSYS Fluent’s built in CAD software, DesignModeler, the shapes shown in Fig. 2 were merged to form the uncoiled aneurysm geometry (Fig. 3). The green line in Fig. 3 shows the additional line necessary to create the geometry for the coiled case, as for this case the aneurysm and the blood vessels were separated into two surfaces.

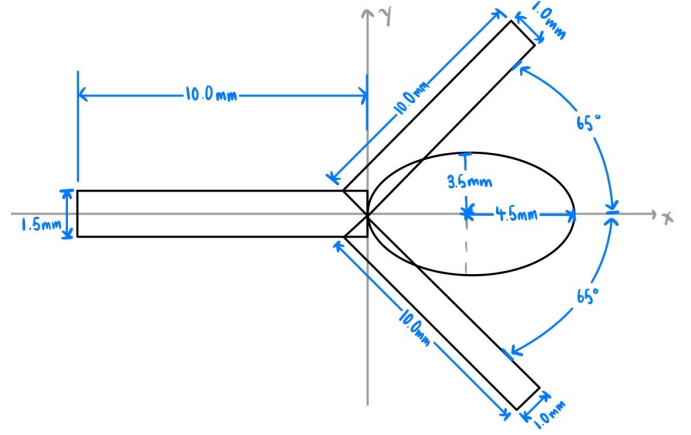


Fig. 2. Dimensioned aneurysm geometry

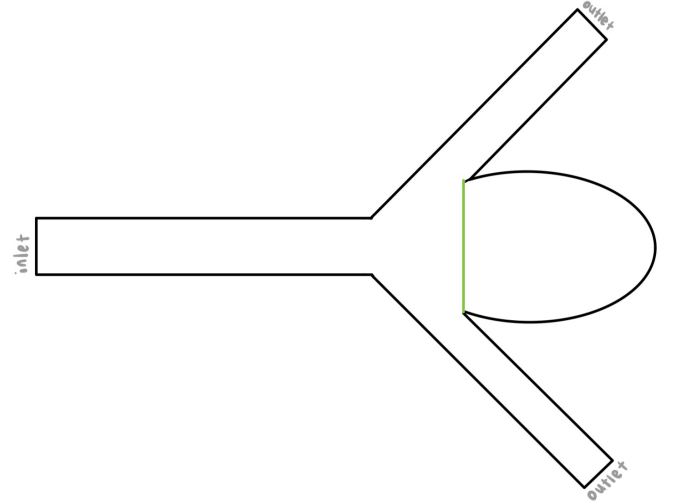


Fig. 3. Aneurysm geometry (Extra green construction line only for coiled case)

### 3) Create Mesh

The geometry was then meshed, with elements of size 0.00011m (justification for sizing explained in Numerical Methods: Grid Independence). The mesh is unstructured and triangular.

### 4) Define Boundary Conditions and Parameters

The boundary conditions and parameters for this simulation, given by the assignment manual [12] are as follows:

- Blood mass density,  $\rho_{\text{Blood}} = 1060 \text{ kg/m}^3$
- Dynamic viscosity,  $\mu = 0.00357 \text{ kg/m}\cdot\text{s}$
- Inlet velocity,  $v_{\text{inlet}} = 0.27 \text{ m/s}$

In addition, for the coiled cases, the following parameters are necessary to define the porous aneurysm region:

- Viscous Resistance =  $1e8$
- Porosity = 0.7

Finally, for the non-Newtonian cases, the following parameters are required:

- Power law index,  $n = 0.4815$

- Flow consistence index,  $k = 0.2073 \text{ kg}\cdot\text{s}^{-1.5185}/\text{m}$
- Minimum viscosity limit =  $0.003 \text{ kg}/\text{m}\cdot\text{s}$
- Maximum viscosity limit =  $0.0125 \text{ kg}/\text{m}\cdot\text{s}$

### 5) Solver Methodology

For all simulations, all residuals were set to an absolute criteria of  $1e-18$ . The solution method was set to a coupled pressure-velocity scheme, and the spatial discretization for pressure and momentum were set to second order and second order upwind, respectively. Each simulation was 'hybrid initialized' 30 times and run for a total of 4000 iterations in order to ensure convergence.

## III. RESULTS AND DISCUSSION

### A. Grid Independence

Table I below displays the results of the grid independence study.

Table I: Results of grid independence study

Mesh Element Size (m)	No. of Mesh Elements	Outlet Velocity (m/s)	Ave. Static Pressure (Pa)	Ave. WSS (Pa)
0.00100	184	0.2190	71.3180	1.9818
0.00090	226	0.2221	71.5291	1.9569
0.00080	305	0.2207	79.4819	2.5600
0.00070	401	0.2153	83.2913	2.5742
0.00060	494	0.2177	83.3646	2.6652
0.00050	712	0.2280	80.8907	2.9149
0.00040	1080	0.2271	88.0933	3.1852
0.00030	1867	0.2257	88.1146	3.4126
0.00020	4537	0.2289	89.5870	3.6401
0.00019	5022	0.2253	87.2310	3.6581
0.00018	5360	0.2278	88.0226	3.6118
0.00017	6070	0.2278	88.1150	3.6296
0.00016	6736	0.2268	89.9354	3.6747
0.00015	7750	0.2277	90.8310	3.6751
0.00014	9042	0.2246	91.8095	3.7005
0.00013	10359	0.2275	89.6923	3.6825
0.00012	11848	0.2262	91.4054	3.6864
0.00011	14239	0.2283	90.3425	3.7117
0.00010	17233	0.2267	90.0293	3.7433
0.00009	21600	0.2262	89.7506	3.7292
0.00008	27164	0.2264	90.5301	3.7302
0.00007	34882	0.2259	90.1461	3.7667

The number of mesh elements was varied by changing the mesh element size. Initially, the range in mesh element size was varied from  $0.0001\text{m}$  to  $0.001\text{m}$  in increments of  $0.0001\text{m}$ . However, due to insignificant variations in results from  $0.0002\text{m}$  to  $0.0001\text{m}$ , the study was extended to explore mesh element sizes in ranges  $0.00007$  to  $0.0002$  in increments of  $0.00001\text{m}$ .

The dependent variables were then plotted against the Number of Mesh Elements, as shown in Fig. 4, 5 and 6. In each graph, the point after which there appears to be no significant variations in results is boxed in red.

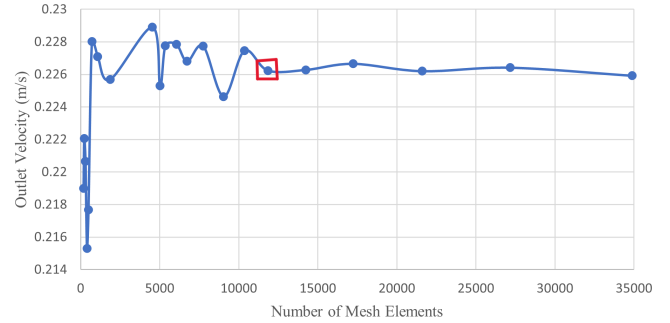


Fig. 4. Outlet velocity vs. number of mesh elements

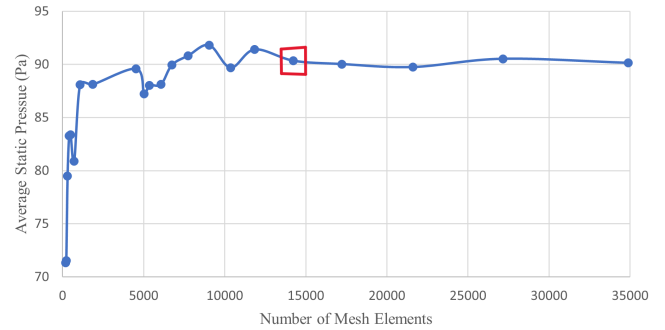


Fig. 5. Average static pressure vs. number of mesh elements

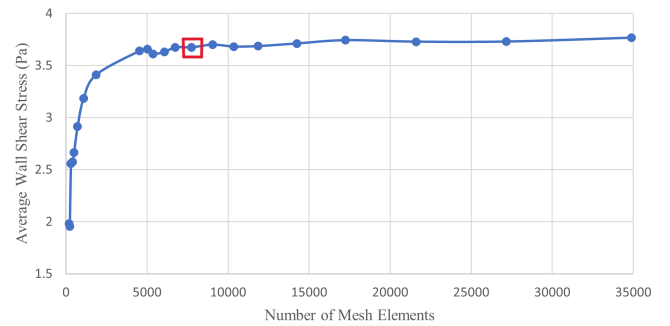


Fig. 6. Average WSS vs. number of mesh elements

The ideal number of mesh elements for the simulation was taken to be the lowest value for all three variables to have stabilized, 14239. This corresponds to a mesh element size of  $0.00011\text{m}$ .

### B. Velocity Magnitude

Fig. 7 and 8 illustrate path line plots of the velocity magnitude within the cerebral aneurysm for the Newtonian coiled and uncoiled cases.

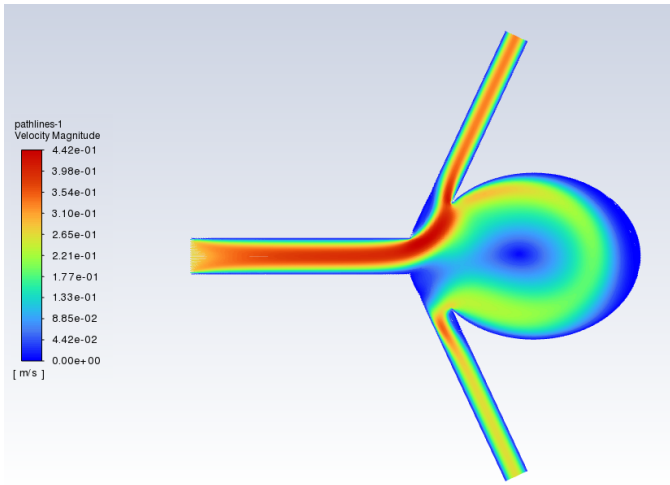


Fig. 7. Path line plot of velocity magnitude in an **uncoiled** cerebral aneurysm with **Newtonian** flow [ANSYS Fluent generated image]

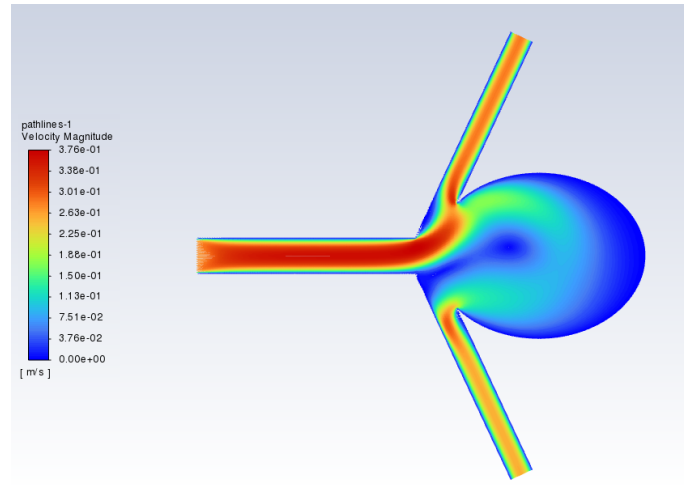


Fig. 9. Path line plot of velocity magnitude in an **uncoiled** cerebral aneurysm with **non-Newtonian** flow [ANSYS Fluent generated image]

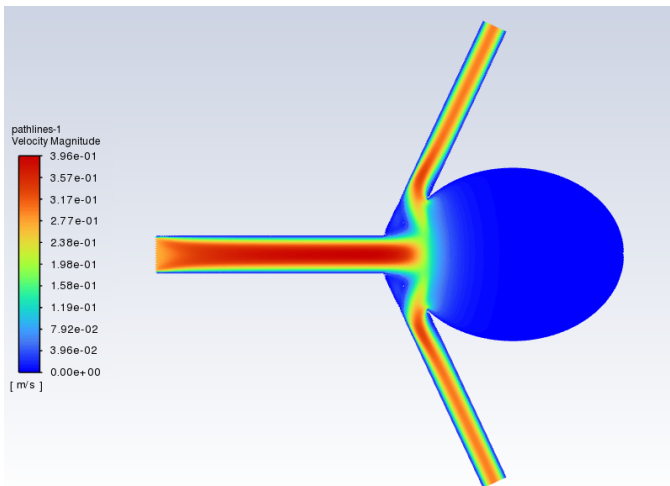


Fig. 8. Path line plot of velocity magnitude in a **coiled** cerebral aneurysm with **Newtonian** flow [ANSYS Fluent generated image]

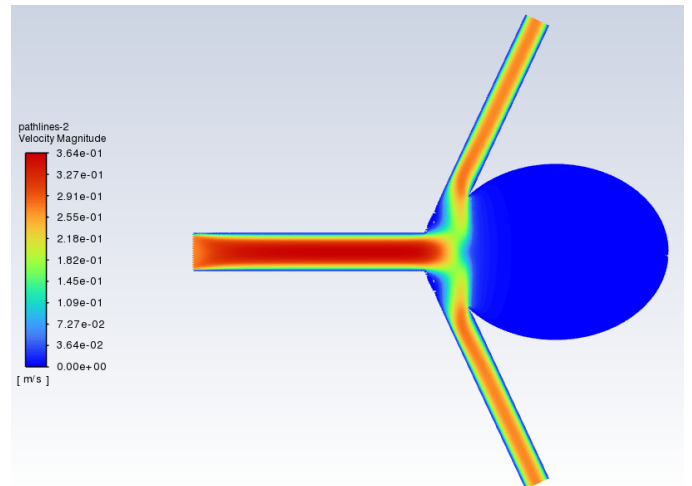


Fig. 10. Path line plot of velocity magnitude in a **coiled** cerebral aneurysm with **non-Newtonian** flow [ANSYS Fluent generated image]

Prior to coil embolization, there appears to be eddy-like flow within the aneurysm (Fig. 7). This circular flow exerts a force on the aneurysm walls and could be a cause for aneurysm growth. After coiling, there is a significant reduction of flow speed within the aneurysm, from approximately 0.221m/s (comparable to the inlet velocity) to almost 0m/s (Fig. 8). The circular currents also disappear. However, this leads to a significant increase in flow speed through the vascular branches at the bifurcation.

Fig. 9 and Fig. 10 depict path line plots of the velocity magnitude for the non-Newtonian coiled and uncoiled cases.

For the uncoiled cases, the flow near the blood vessel walls is *faster* for the non-Newtonian case (Fig. 9) than the Newtonian case (Fig. 7). This can be explained by the pseudoplastic nature of blood; blood experiences a higher shear force closer to the wall, so it becomes less viscous and can flow faster.

In contrast, the flow in the aneurysm is *slower* for the non-Newtonian uncoiled case than for the Newtonian uncoiled case. This is because when the blood exits the main vasculature branch into the opening of the aneurysm, its viscosity increases, thus slowing its flow.

After coiling, the flow within the aneurysm is significantly reduced for both the non-Newtonian (Fig. 10) and the Newtonian (Fig. 8) cases. According to low-flow theory, this could be a concerning effect and could induce aneurysm rupture.

### C. Wall Shear Stress

Fig. 11 and 12 illustrate plots of the WSS along the curve length of the aneurysm wall for the Newtonian coiled and uncoiled cases.

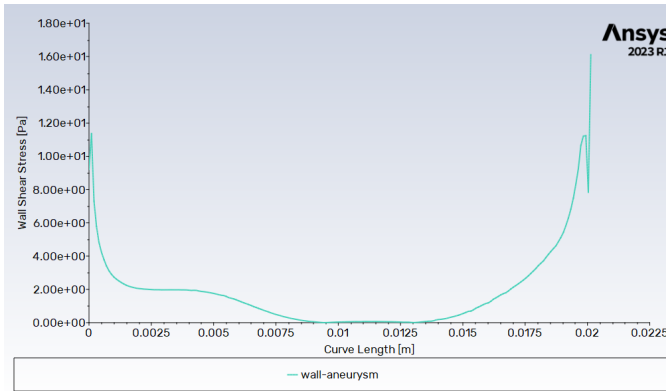


Fig. 11. WSS along aneurysm wall for an **uncoiled** cerebral aneurysm with **Newtonian** flow [ANSYS Fluent generated image]

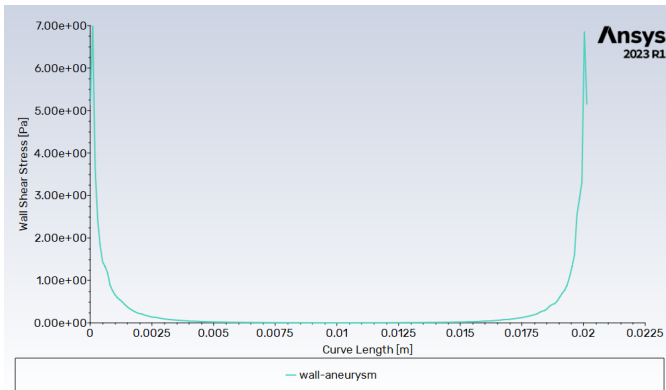


Fig. 12. WSS along aneurysm wall for a **coiled** cerebral aneurysm with **Newtonian** flow [ANSYS Fluent generated image]

In Fig. 11, the WSS is 0 Pa from a curve length of 0.0090m to 0.0135m; this is because this region is the base of the aneurysm (i.e. the green line in fig. 3) and has no physical wall. For this region, this section of curve length will be 0 Pa for all graphs.

In Fig. 11, prior to coiling, the WSS seems to increase exponentially along the aneurysm wall, reaching a maximum of approximately 16 Pa at the point furthest from the aneurysm base. Regions of high WSS indicate a potential high risk of rupture. However, in reality, the thickness of the aneurysm wall is not constant; a thin-walled region may be more susceptible to rupture, even if it is not at the point of maximum shear stress.

When coiled, the WSS is significantly decreased, and most regions experience an almost negligible shear stress. The maximum WSS is decreased to approximately 7 Pa; this is a significant reduction by 56.25%.

Fig. 13 and 14 below depict plots for WSS against the aneurysm curve length for the non-Newtonian uncoiled and coiled cases.

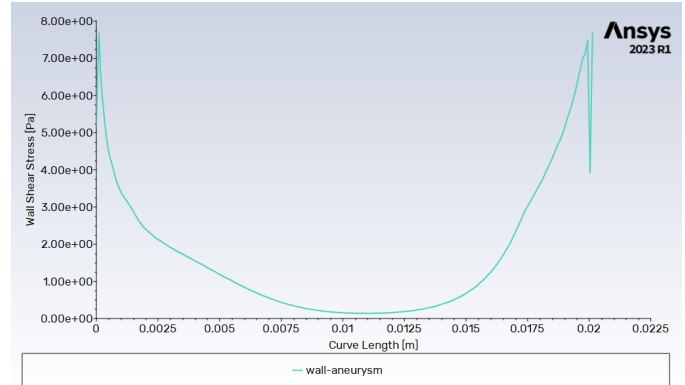


Fig. 13. WSS along aneurysm wall for an **uncoiled** cerebral aneurysm with **non-Newtonian** flow [ANSYS Fluent generated image]

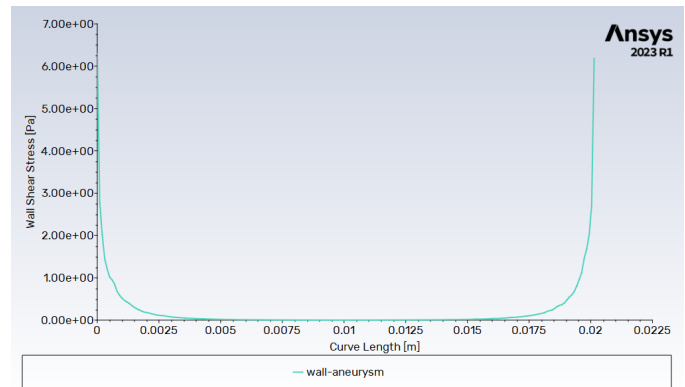


Fig. 14. WSS along aneurysm wall for a **coiled** cerebral aneurysm with **non-Newtonian** flow [ANSYS Fluent generated image]

When simulated with a non-Newtonian fluid, the maximum WSS prior to coiling is only 7.8 Pa, notably less than when simulated using a Newtonian fluid. Again, this is likely a result of the pseudoplastic nature of the simulated blood: as blood becomes less viscous near the walls it exerts a lower shear stress on the walls. After coiling, the maximum WSS is only reduced to 6.2 Pa. Nonetheless, the reduction would theoretically reduce high-flow effects which contribute to aneurysm rupture. Further explorations would need to be conducted to determine what range of WSS values can be deemed safe from causing rupture.

### D. Static Pressure

Fig. 15 and 16 below show contour plots of the static pressure within the aneurysm for Newtonian flow, both coiled and uncoiled.

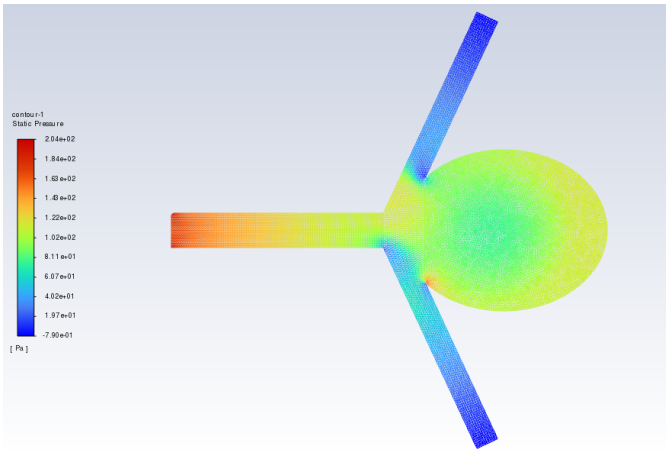


Fig. 15. Static pressure contour plot of an **uncoiled** cerebral aneurysm with **Newtonian** flow [ANSYS Fluent generated image]

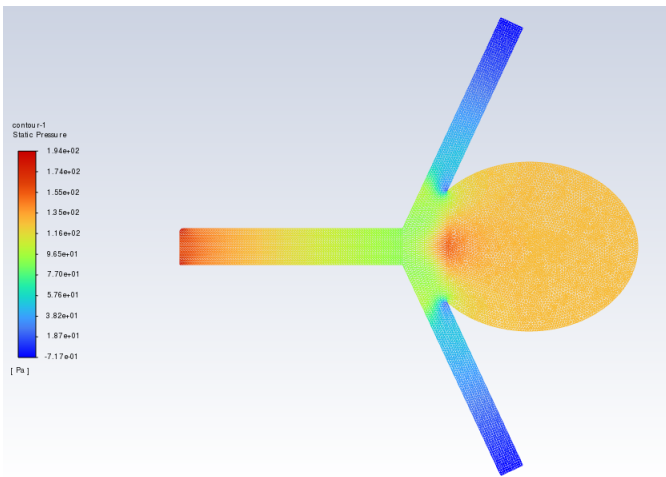


Fig. 16. Static pressure contour plot of a **coiled** cerebral aneurysm with **Newtonian** flow [ANSYS Fluent generated image]

The pressure is the highest at the inlet, and the lowest at the outlets. Interestingly, for the Newtonian case, the maximum intra-aneurysmal pressure increases after the deployment of a coil, from approximately 102 Pa to 135 Pa. This is an undesirable result, as hypertension (high blood pressure) has been linked to higher risks of aneurysm rupture [14]. However, it is important to note that in this model, the walls are rigid and unable to recoil. In actuality, the walls may be able to expand to accommodate for changes in pressure.

Fig. 17 and 18 below show similar contour plots, but for the non-Newtonian flow.

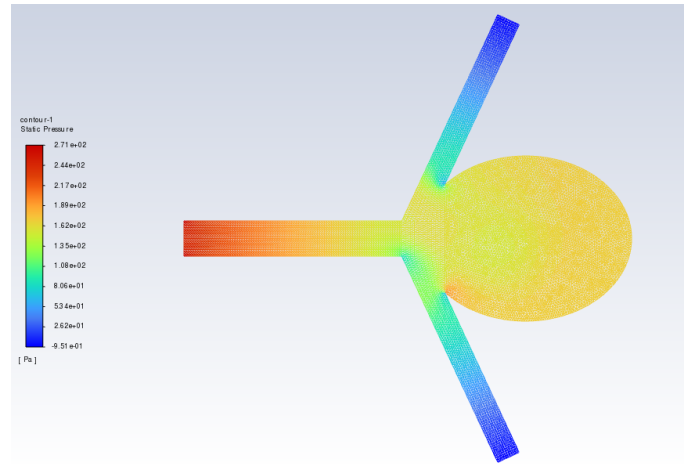


Fig. 17. Static pressure contour plot of an **uncoiled** cerebral aneurysm with **non-Newtonian** flow [ANSYS Fluent generated image]

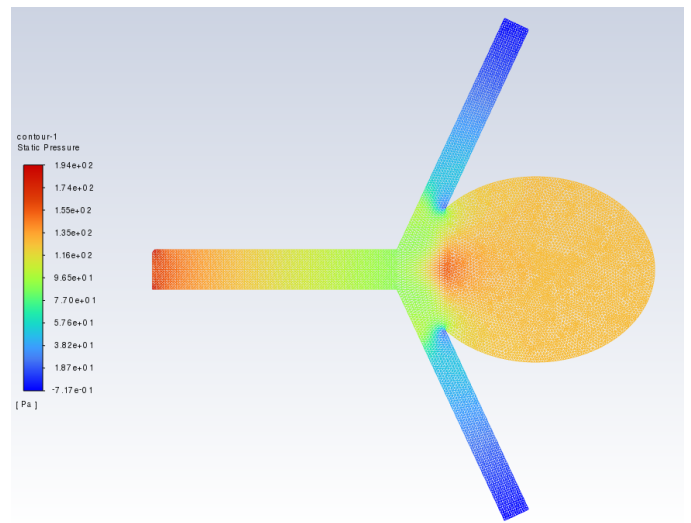


Fig. 18. Static pressure contour plot of a **coiled** cerebral aneurysm with **non-Newtonian** flow [ANSYS Fluent generated image]

For this case, the intra-aneurysmal pressure had a completely opposite change when coiled: it decreased, from approximately 162 Pa to 135 Pa. It can be argued that the non-Newtonian results are more accurate, as its properties are more similar to that of blood. Thus, the conclusion can be made that coiling can reduce the intra-aneurysmal pressure. However, further studies should be done to confirm this result.

#### IV. CONCLUSIONS AND FUTURE WORK

To conclude, the use of an endovascular coil as a form of treatment for cerebral aneurysms has a significant effect on the intra-aneurysmal haemodynamic properties. As a result of coiling, the WSS is decreased, reducing high-flow effects. The intra-aneurysmal static pressure also decreases (when modelled with a non-Newtonian fluid), reducing high-flow

effects. However, the velocity profile is stagnated within the aneurysm, contributing to low-flow effects, a potentially concerning result.

As coiling reduces high flow effects but also increases low flow effects, the net result depends which effect contributes greater to aneurysm rupture. Further research, perhaps with real, experimental patient data, is required to draw these conclusions.

Furthermore, the use of Newtonian blood rheology as opposed to non-Newtonian generates drastically different results, as observed for all haemodynamic variables. The non-Newtonian results seem to align more closely with research, thus are more reliable. To improve the simulation and make the results more accurate, the model could be created with flexible walls, as this appears to be a main limitation of the study. Additionally, the inlet velocity could be modelled as a function of time to account for the variations in velocity between periods of systolic and diastolic blood pressure (pulsatile haemodynamics). The model could also be created in 3D, as this would generate a more complete picture of the system.

In addition, it is important to note that the causes of aneurysm rupture are not purely mechanical. Biological factors such as genetics, age, and race have an equally significant role on aneurysm behavior. It is an overgeneralization to create one simple geometry and draw conclusions which can be applied to all patients. A more detailed study would simulate each patient's case individually, as the biological factors and the aneurysm geometry would differ on a case to case basis.

Research suggests that a coil packing density of 24% or greater [15] is ideal. To continue this study, it would be interesting to investigate how changing the coil packing density, i.e. the porosity of the aneurysm, affects the haemodynamics within the aneurysm. Additionally, it would be worthwhile to study how changing the geometry of the model impacts the effectiveness of endovascular coiling. Some geometrical factors include the angle of the bifurcation, the size of the aneurysm, and the width of the attached blood vessels. Moving forward, the continuation of this research will play a vital role in forming a complete understanding the behavior of cerebral aneurysms and the causes of their rupture.

## REFERENCES

- [1] Sforza, Daniel M., et al. "Hemodynamics of cerebral aneurysms." *Annual Review of Fluid Mechanics*, vol. 41, no. 1, 2009, pp. 91–107, <https://doi.org/10.1146/annurev.fluid.40.111406.102126>.
- [2] "NHS Overview: Brain Aneurysm." *NHS*, NHS, [www.nhs.uk/conditions/brain-aneurysm/](http://www.nhs.uk/conditions/brain-aneurysm/). Accessed 14 Nov. 2023.
- [3] "Cerebral Aneurysms." *National Institute of Neurological Disorders and Stroke*, U.S. Department of Health and Human Services, [www.ninds.nih.gov/health-information/disorders/cerebral-aneurysms#:~:text=The%20bulging%20aneurysm%20can%20put,%2C%20coma%2C%20and%20even%20death](http://www.ninds.nih.gov/health-information/disorders/cerebral-aneurysms#:~:text=The%20bulging%20aneurysm%20can%20put,%2C%20coma%2C%20and%20even%20death.). Accessed 14 Nov. 2023.
- [4] "Coil Embolization for Brain Aneurysms." *Atlanta, GA - Spine Surgery*, Atlanta Spine Institute, 9 July 2020, [atlantaspineinstitute.com/cranial-treatment-options/coil-embolization-for-brain-aneurysm/](http://atlantaspineinstitute.com/cranial-treatment-options/coil-embolization-for-brain-aneurysm/).
- [5] Sforza, Daniel M., et al. "Computational fluid dynamics in brain aneurysms." *International Journal for Numerical Methods in Biomedical Engineering*, vol. 28, no. 6–7, 2011, pp. 801–808, <https://doi.org/10.1002/cnm.1481>.
- [6] UCL MECH0059 CFD Lecture 2 Slides.
- [7] "Anatomy and Physiology II." *Structure and Function of Blood Vessels / Anatomy and Physiology II*, Lumen Learning & OpenStax, [courses.lumenlearning.com/suny-ap2/chapter/structure-and-function-of-blood-vessels/](https://courses.lumenlearning.com/suny-ap2/chapter/structure-and-function-of-blood-vessels/). Accessed 14 Nov. 2023.
- [8] Umeda, Yasuyuki, et al. "Computational Fluid Dynamics (CFD) using porous media modeling predicts recurrence after coiling of cerebral aneurysms." *PLOS ONE*, vol. 12, no. 12, 2017, <https://doi.org/10.1371/journal.pone.0190222>.
- [9] Billen, Magali. "2.5: Darcy's Law - Flow in a Porous Medium." *Geosciences LibreTexts*, Libretexts, 6 Feb. 2021, [geo.libretexts.org/Courses/University\\_of\\_California\\_Davis/GEL\\_056%3A\\_Introduction\\_to\\_Geophysics/Geophysics\\_is\\_everywhere\\_in\\_geology.../02%3A\\_Diffusion\\_and\\_Darcy%27s\\_Law/2.05%3A\\_Darcy%27s\\_Law\\_-\\_Flow\\_in\\_a\\_Porous\\_Medium](https://geo.libretexts.org/Courses/University_of_California_Davis/GEL_056%3A_Introduction_to_Geophysics/Geophysics_is_everywhere_in_geology.../02%3A_Diffusion_and_Darcy%27s_Law/2.05%3A_Darcy%27s_Law_-_Flow_in_a_Porous_Medium).
- [10] "Pseudoplastic Fluid." *ScienceDirect Topics*, [www.sciencedirect.com/topics/engineering/pseudoplastic-fluid](https://www.sciencedirect.com/topics/engineering/pseudoplastic-fluid). Accessed 14 Nov. 2023.
- [11] Ballyk PD, Steinman DA and Ethier CR. (1994). Simulation of Non-Newtonian Blood Flow in an End-to-Side Anastomosis, *Biorheology*, 31: 565–586.
- [12] UCL MECH0059 Assignment Manual, Computational Modelling of the Haemodynamics in Coiled and Uncoiled Cerebral Aneurysms
- [13] *ANSYS Tutorial | Grid Independence Test In ANSYS Fluent Using Parametric Analysis*, ANSYS-Tutor, 24 Aug. 2019, <https://www.youtube.com/watch?v=D9mVeqfIU8g>. Accessed 14 Nov. 2023.
- [14] Tada, Yoshiteru, et al. "Roles of hypertension in the rupture of intracranial aneurysms." *Stroke*, vol. 45, no. 2, 2014, pp. 579–586, <https://doi.org/10.1161/strokeaha.113.003072>.
- [15] Osuga, Keigo, and Taku Yasumoto. "Packing Density Considerations for True Visceral Aneurysms." *Endovascular Today*, Bryn Mawr Communications, 27 Aug. 2014, [evtoday.com/articles/2014-aug/packing-density-considerations-for-true-visceral-aneurysms#:~:text=Tight%20coil%20packing%20of%20saccular,to%20achieve%20adequate%20coil%20packing](http://evtoday.com/articles/2014-aug/packing-density-considerations-for-true-visceral-aneurysms#:~:text=Tight%20coil%20packing%20of%20saccular,to%20achieve%20adequate%20coil%20packing).